Proceedings 10th NUMGE 2023
10th European Conference on Numerical Methods in Geotechnical Engineering
Zdravkovic L, Kontoe S, Taborda DMG, Tsiampousi A (eds)

https://doi.org/10.53243/NUMGE2023-114

Impact of undrained induced anisotropy on the liquefaction resistance of sand

M. Tafili[1], T. Wichtmann[1]

[1]*Chair of Soil Mechanics, Foundation Engineering and Environmental Geotechnics, Ruhr-University Bochum, Bochum, Germany*

ABSTRACT: This study focuses on the impact of undrained loading on the development of strains and excess pore water pressure in granular materials and its effect on the liquefaction resistance of the soil. The research was conducted using a combination of both, laboratory tests and numerical simulations. Therefore, saturated samples were subjected to small or large (cyclic) stresses in triaxial extension and compression until the pore water pressures increased to specific values, but not resulting in a complete loss of the mean effective stress. To investigate the influence of undrained preloading, after reconsolidation the sample was further subjected to a second cyclic drained or undrained loading with the same magnitude. The results of the study show that undrained loading can induce anisotropy in sand and that this anisotropy can have a significant impact on the liquefaction resistance as well as accumulation of strains of the soil. Depending on the magnitude of the undrained or drained subsequent shearing, the preloading may result in increasing or decreasing liquefaction resistance of soil. Furthermore, the sample subjected to large preshearing on one side of triaxial loading, became stiffer on that side, but softer on the opposite side. The reproducibility of these dependencies is investigated with the Sanisand model, which is a widely used and well-established tool for the analysis of soil behaviour.
The findings of the study have important implications for the design and analysis of structures founded on sand with advanced constitutive models, particularly in areas prone to earthquakes or other seismic events.

Keywords: sand; preloading; cyclic loading; preshearing; Sanisand

1 INTRODUCTION

Preloading and preshearing present two techniques used in geotechnical engineering to increase the liquefaction resistance of sand. Preloading involves applying an initial load to soil before for example a seismic event, with the aim to increase the effective stress of the soil and improve its strength and stiffness. Preshearing involves the application of a shear stress to soil prior to another loading event, which may increase the soil's strength and stiffness. These techniques have practical implications in the design and construction of foundations, embankments, and other structures built on sandy soils. They are also important in the assessment and mitigation of seismic hazard in areas prone to liquefaction. Additionally, they are also used in the mining industry to stabilize slopes and in coastal engineering to protect against soil liquefaction during tsunamis.

The use of preloading and preshearing can help to reduce the potential for damage and failure of structures during earthquakes, making them safer for the public and more resilient to natural disasters. While a densification of the sandy soil during preloading is expected as a time-efficient process, the limitations of preloading and surcharging in clayey soils is exactly the long-lasting consolidation or pore water pressure dissipation. Further limitations of the preloading present the excessive lateral deformation of the pre-compression fill, often because of the transmission of high excess pore water pressure.

The preshearing influence on the behaviour of a soil is, however, not always positive and it depends on whether it involves large or small shear strains (Ishihara and Okada, 1987; Knittel et al., 2023). According to various studies in the literature, including Finn et al. (1970), Suzuki and Toki (1989), Liu et al. (2021), Tafili et al. (2022), liquefaction resistance is typically increased during a second undrained phase after reconsolidation when the preloading history is made up of cycles that are either drained or undrained implying small strain amplitudes. This results primarily from the hardening phenomenon due to plastic yielding, which is expected to be reproduced well by advanced constitutive models such as Sanisand (Dafalias and Manzari, 2004). On the other hand, preshearing involving deviatoric stress amplitudes leading to large shear strains tends to cause the sand to liquefy easily (Finn et al., 1970; Ishihara and Okada, 1987). Such reduction is sometimes also observed in situ, when a re-liquefaction of the sand occurs during an after-shock event with smaller intensity than the main earthquake (Knittel et al., 2023).

Ishihara and Okada (1987) tested the Fuji river sand documenting that after large preshearing, although with a lower void ratio, the sample shows liquefaction in the first cycle of the second cyclic loading, while in the first cyclic loading it could withstand many cycles. Hence, the undrained preloading history may reduce the resistance against liquefaction. The role of preshearing on the mechanical behaviour of granular materials will be recalled and summarized in this paper.

Constitutive soil models have shown to be an effective numerical tool for simulating soil behaviour. Therefore, these experiments will be numerically analyzed in the course of the paper. In order to reach a wide audience, the simulations will be performed with the widely applied Sanisand model of Dafalias and Manzari (2004). Thus, among other discussions, it will be made possible to identify the applications for which the model is more suitable. This is crucial for the application of advanced constitutive models in geotechnical engineering practice.

2 TEST MATERIAL AND DEFINITIONS

The Fuji river sand used by Ishihara and Okada (1987) has a subangular grain shape with a specific gravity of SG=2.73, a mean particle size of $d_{50} = 0.38$ mm and a uniformity index of $C_u = 2.21$. The minimum and maximum void ratios were determined as $e_{min} = 0.53$ and $e_{max} = 1.08$, respectively.

The terms "large" and "small" preshear, which will be used throughout the paper, refer to the amount of strain or deformation that is applied to the material before the main loading (second or third load of the test) begins. In a "large" preshear, a significant amount of strain is applied to the material, whereas in a "small" preshear, only a small amount of strain is applied. Figure 2 illustrates the effective stress path (curve ABC) of a medium dense to dense sand sample subjected to undrained shearing until failure. The straight line from the origin passing through the point B is denoted as phase transformation line (PTL, Ishihara et al., 1975). This line separates the area with decreasing mean effective stress (increasing excess pore water pressure) from the domain characterized by an increase in both the mean effective stress and the deviatoric stress. On one side of the PTL (path AB, range of small preshearing), the soil exhibits solid-like behaviour and follows a typical stress-strain relationship with small generation of deformation, whereas on the other side (path BC, range between PTL and failure line), the soil exhibits fluid-like behaviour and is characterized by large changes in strain. Hence, a preloading condition where the variation in effective stress crosses the PTL is denoted in the following as large preshearing.

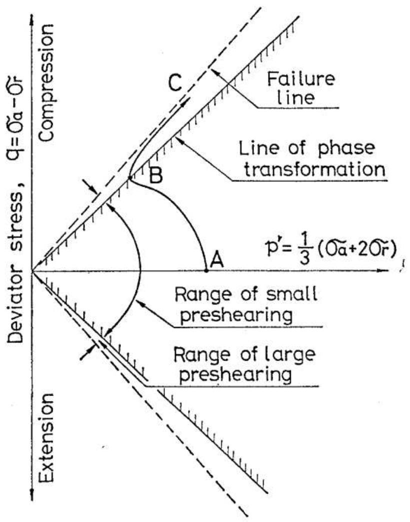

Figure 2. Illustration for small and large preshearing from Ishihara and Okada (1987)

3 SIMULATIONS VS. EXPERIMENTS

In the following, the experimental results of Fuji river sand (Ishihara and Okada, 1987) will be discussed in detail along with new simulation results with Sanisand. The tests comprise in total 4 cyclic triaxial tests with small and large (cyclic) undrained preloading, reconsolidation to the initial state and subsequent undrained cyclic triaxial stress paths. For this purpose, the Sanisand model proposed by Dafalias and Manzari (2004), which is a widely used and well-established tool for the analysis of soil behaviour and is a valuable resource for geotechnical engineers working in the field of soil mechanics and geohazard engineering is used. The simulations are performed with Incremental Driver, a single element code developed by Andrzej Niemunis (2007, 2014, 2023) for running element tests using constitutive models implemented in umat format.

Due to the lack of experiments involving Fuji river sand subjected to monotonic loading, the Sanisand parameters, which have been calibrated using a comprehensive database of Karlsruhe fine sand (KFS) in prior studies by Wichtmann and Triantafyllidis (2016), will be utilized for simulation purposes. The parameter values used for the numerical analysis are taken from Wichtmann et al. (2019) and are listed in Table 1.

Table 1. Material parameters of Sanisand for Karlsruhe fine sand (Wichtmann et al., 2019)

e_0	λ	ξ	M_c	M_e	m	G_0
1.103	0.122	0.205	1.34	0.938	0.05	150
h_0	c_h	n_b	A_0	n_d	z_{max}	c_z
10.5	0.75	1.2	0.9	2.0	20	10000

3.1 *Small preshearing*

Figure 3 presents an undrained cyclic triaxial test with a deviatoric stress amplitude of $q^{ampl} = 40$ kPa, whereby the first cyclic loading achieved N=3 cycles until an excess pore water pressure of approx. 45% of the initial effective confining pressure. Then, the sample was reconsolidated to the initial effective confining pressure (corresponding to the one before the first cyclic loading) and again cyclic undrained loading with the same deviatoric amplitude until N=2 cycles is applied. The change in the relative density of the sample between first ($D_{r0} = 47.1\%$) and second ($D_{r0} = 48\%$) cyclic loading is marginal, hence the change in void ratio, is negligible as well. The pore water pressure build-up in the second cyclic loading corresponds to approx. 11% compared to approx. 40% after N=2 cycles during first cyclic loading, see Figure 3a. Even though the simulation presents qualitatively the same trend, quantitatively the reduction rate of pore water pressure build-up in the second cyclic loading is much lower. The difference between first and second loading is approx. 5% compared to approx. 29% in the experiment. The stress-strain relationship rendered by the simulations is depicted in Figure 3b, whereas smaller axial strain was developed in the second loading. Summarising, the preloading with this small deviatoric amplitude led to a workhardening of the sample in the laboratory, which is to some extent realistically reproduced with the model.

Figure 4 presents a test with the same deviatoric stress amplitude but with increasing number of cycles in the first loading, specifically N=4.5 cycles until a development of approx. 70% excess pore water pressure have been applied. Regardless of the number of cycles applied during the first loading, a comparison of the effective stress paths depicted in Figure 4a and Figure 3a demonstrates that the behaviour of the sample during the second cyclic loading in both the laboratory and Sanisand simulation results in almost equivalent levels of pore water pressure build-up. Hence, now the experiment shows an approx. 6 times higher reduction of the rate of excess pore water pressure between first and second loading than the simulation. Nevertheless, the simulation succeeds in reproducing the higher workhardening of the sample with increasing N resulting in a higher reduction of pore water pressure generation when compared between first and second loading at the same cycle. For both tests the relative densities prior to the cyclic loading sequencies were almost similar, such that the change in the mechanical behaviour cannot be attributed to a densification of the sample. Hence it can be concluded, that if a sand sample is subjected to a sequence of small amplitude of shear stresses in undrained conditions, developing some amount of pore water pressure, the sample develops workhardening and, as a result, after it is consolidated again and sheared upon the same stress amplitude, the development of axial strains is reduced.

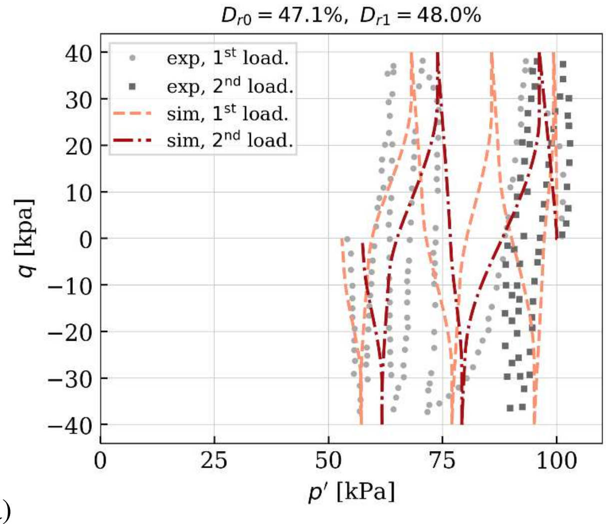

a)

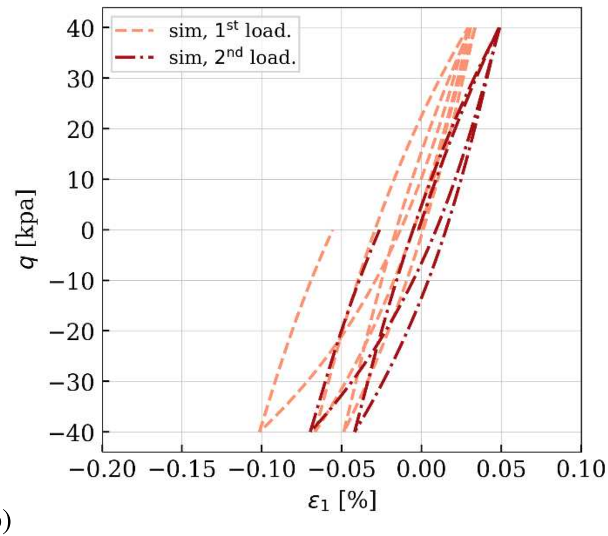

b)

Figure 3. Behaviour of Fuji river sand subjected to small cyclic preshear (digitized from Ishihara and Okada, 1978) and simulations with Sanisand

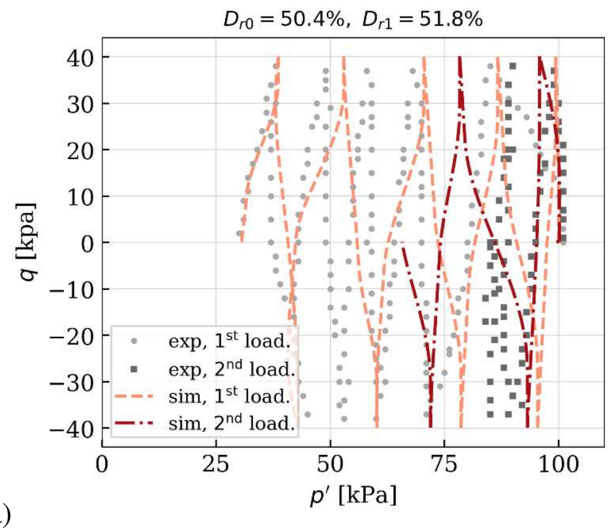

a)

Figure 4. Behaviour of Fuji river sand subjected to small cyclic preshear (digitized from Ishihara and Okada, 1978) and simulations with Sanisand

3.2 Large preshearing

Figure 5 presents a medium dense sample subjected to a first cycle with a deviatoric stress amplitude of $q^{ampl} \approx 40$ kPa followed by a large deviatoric stress of $q = 90$ kPa (surpassing the phase transformation line) in triaxial compression. The 1st load resulted in an excess pore water pressure of 62.5% of the initial effective confining pressure. Afterwards, the sample was reconsolidated to the same initial effective confining pressure and subjected to a second cyclic loading with the same magnitude and sequence as the first load. The effective stress path of the second load indicates a reduction in the build-up of excess pore water pressure of approx. 25% in the experiment, even though there is no significant change in relative density. Although the simulation with Sanisand shows qualitatively a similar behaviour, the reduction of the excess pore water pressure between first and second loading is underestimated by approx. 15%. The stress-strain relationship is presented in Figure 5b, whereas the axial strain in triaxial compression exceeds the strain developed in triaxial extension in both loading paths. This is not in agreement with the experimental results presented by Ishihara and Okada (1987), where the shear strain in triaxial extension far exceeded the shear strain that was induced on the side of triaxial compression. The large experimental difference in the soil behaviour between the triaxial compression and extension was there attributed to the fact that the sample has been precompressed in triaxial compression in the 1st loading making it difficult to deform further in that direction in the 2nd loading. This behaviour is not reproduced by the Sanisand model, which can be observed also in the effective stress path. The simulation develops the highest pore water pressure when subjected to triaxial compressive load (see second cycle of 1st and 2nd load), whereas the experiment experienced the lowest build-up of pore water pressure. In the experiment, loading in triaxial extension in both cyclic loading sequences resulted in the highest rate of excess pore water pressure development.

Figure 6 shows similar experiments and simulations with large preshearing (surpassing the phase transformation line) considering 3 loading sequencies. The sample was first subjected to undrained shearing until approx. $q = 120$ kPa in triaxial compression and then the loading direction was reversed until $q = 0$ kPa was reached. Thereby, a pore water pressure build-up of approx. 66% was reported in the experiment. After reconsolidation, the sample was imposed to a small cyclic loading in triaxial compression with $q^{ampl} \approx 40$ kPa and sheared until $q = 60$ kPa in triaxial extension. The effective stress paths of the experiment presented in Figure 6a evidences a higher pore water pressure development during loading in the direction of triaxial extension. Hence all test results confirm the observance that the preshearing towards a specific triaxial direction makes the sample become stiffer on that side of loading direction but softer on the opposite side. Even though the Sanisand simulation shows a good performance in the prediction of the difference between excess pore water pressure of the 1st and 2nd loading it fails in reproducing the described behaviour in the correct loading direction (triaxial compression or extension). Hence, it develops more pore water pressure when subjected to loading in triaxial compression and produces a higher strain in that direction as well (see Figure 6b).

Following reconsolidation, a third loading was imposed under triaxial compression, with the same magnitude as the first load ($q = 120$ kPa). This loading induced the highest rate of excess pore water pressure and resulted in the largest compressive axial strain observed, surpassing the values obtained during the first load. This behaviour was of course expected, because the sample was imposed to large preshearing in triaxial extension previously, making it softer in the opposite direction. The subsequent shearing until $q = 0$ kPa shows a similar path as the one in the respective first loading. In the third loading, the Sanisand simulation reproduces qualitatively similar trends to those found in the experiment.

3.3 Influence of undrained preshearing on drained cyclic behaviour of KFS

To explore the influence of preshearing on the subsequent soil behaviour, a set of triaxial tests with a combination of undrained preshearing and drained stress cycles is presented in Figure 7. AP1 test without an undrained preshearing history represents the reference starting from an isotropic stress state with an initial mean effective stress $p_0 = 100$ kPa, drained stress paths of length $l_{pq} = \sqrt{p^2 + q^2} = 40$ kPa were investigated under 16 different stress ratios in the compression and extension area. The details of the testing device, sample preparation and further proceeding is described in Knittel et al. (2023). In Test AP2 a small preshearing was conducted, whereas in Test AP3 a large preshearing precedent to the cyclic loading was applied. It can be observed that the magnitude of the preshearing have a major influence on the strain accumulation upon cyclic loading. Simulations of the experiments with Sanisand reveal that the long-lasting effect of preshearing cannot adequately be captured by the model. This deficiency of the constitutive model can lead to unsafe designs due to the overestimation of the cyclic resistance to liquefaction and to the underestimation of long term settlements.

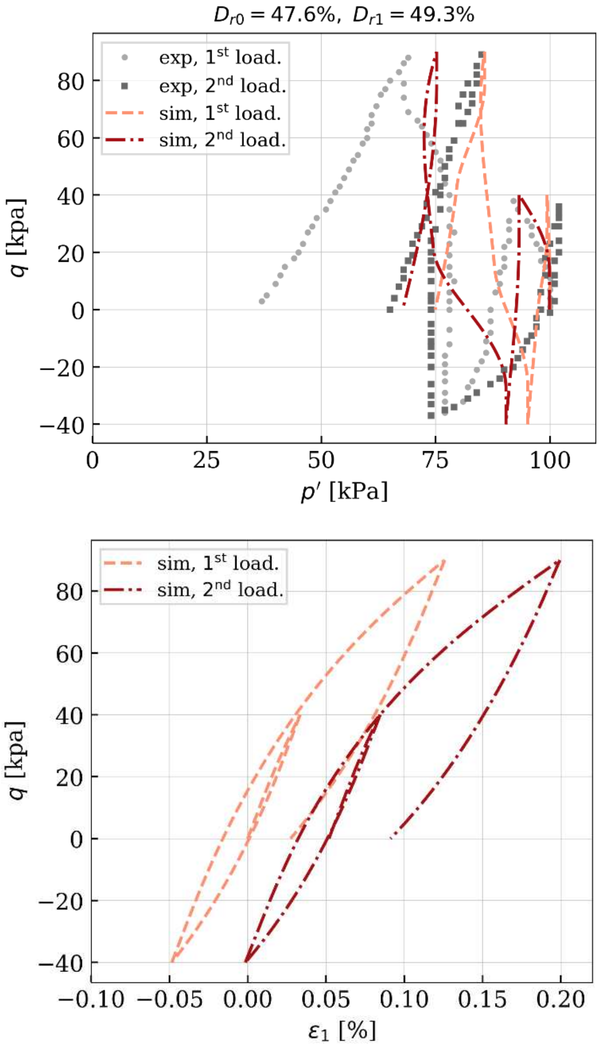

Figure 5. Behaviour of Fuji river sand subjected to large cyclic preshear (digitized from Ishihara and Okada, 1978) and simulations with Sanisand

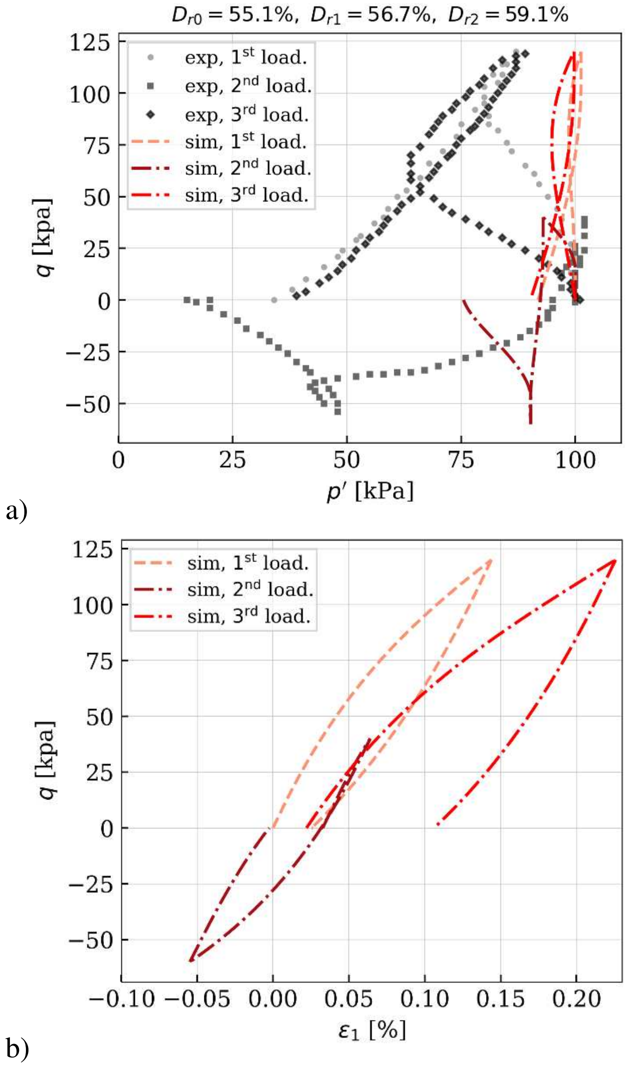

Figure 6. Behaviour of Fuji river sand subjected to large preshear (digitized from Ishihara and Okada, 1978) and simulations with Sanisand

4 CONCLUSIONS

The paper presents the influence of cyclic and monotonic small (before the PTL) as well as large (surpassing the PTL) preshearing on the mechanical behaviour of sand recalling the experiments conducted by Ishihara and Okada (1987) on Fuji river sand. For both types of tests (with small and large preshearing) the relative densities prior to the different loading sequencies were almost similar, such that the change in the mechanical behaviour cannot be attributed to a densification of the sample. The experiments with small preshearing have shown, that if a sand sample is subjected to a sequence of small amplitude of undrained shearing, the sample develops workhardening and, as a result, after it is reconsolidated and sheared upon the same stress amplitude, the development of axial strains and pore water pressure is reduced. These results are qualitatively well reproduced with the considered Sanisand model. In contrary, the samples subjected to large preshearing on a specific side of triaxial loading become stiffer in the direction of shearing and softer on the opposite side. Consequently, the pore water pressure accumulation as well as the development of strains during shearing in the opposite direction increase significantly. The simulations with the Sanisand model show hereby the opposite behaviour, even though the resulting increase in strain and pore water pressure accumulation (after a complete cycle) is qualitatively reproduced well.

5 ACKNOWLEDGEMENTS

The presented study has been funded by the German Research Council (DFG, project No. TR 218/29-1). The authors are grateful to DFG for the financial support.

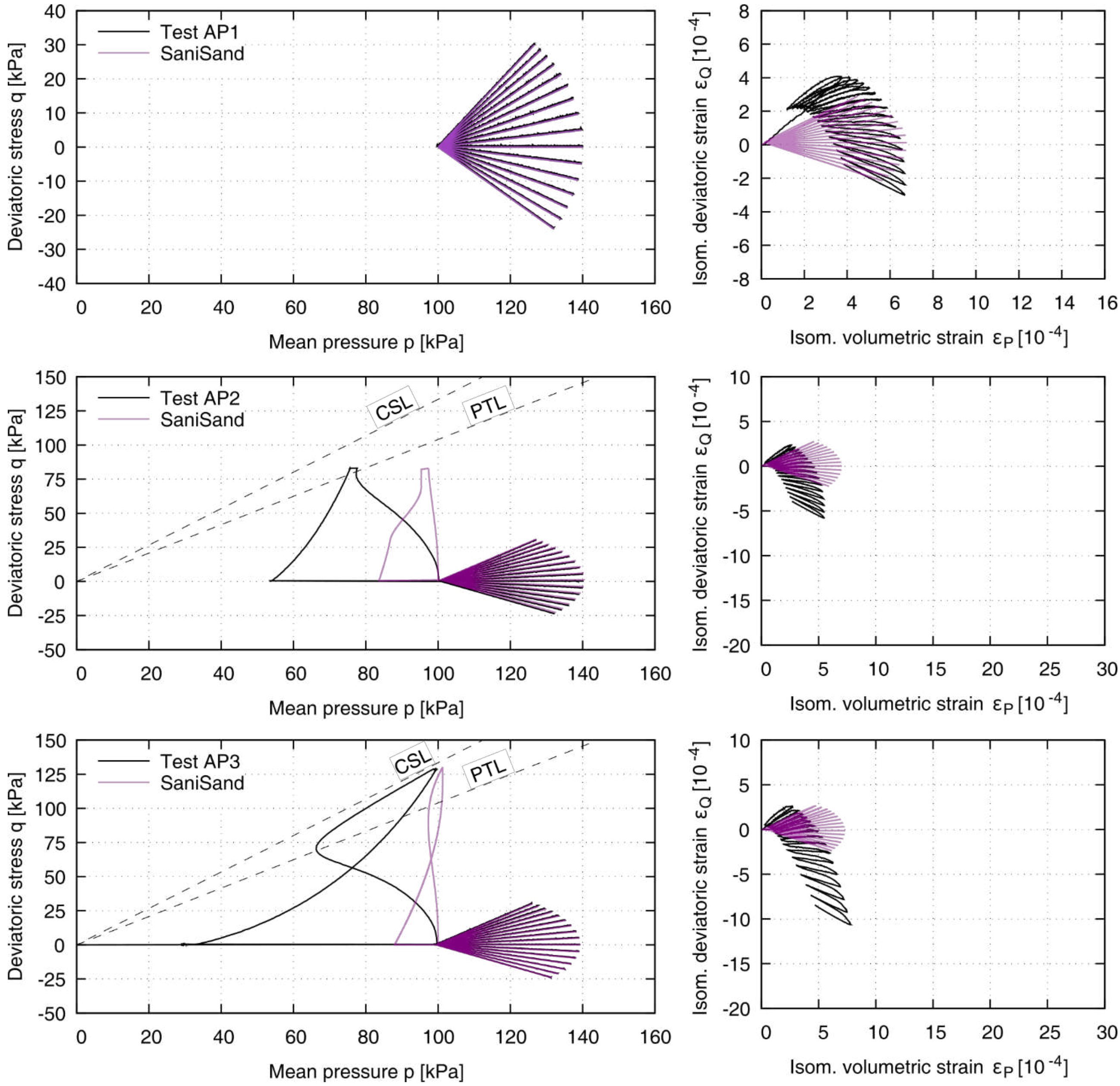

Figure 7. Test results on KFS: a) Test AP1 without preshearing history as reference, b) Test AP2 with small preshearing and c) Test AP3 with large preshearing history.

6 REFERENCES

Dafalias, Y.F., Manzari, M.T. 2004. Simple plasticity sand model accounting for fabric change effects, *J. Eng. Mech.,* **130**(6), 622-634.

Finn, W. L., Bransby, P. L., Pickering, D. J. 1970. Effect of strain history on liquefaction of sand. *Journal of the Soil Mechanics and Foundations Division*, **96**(6), 1917-1934.

Ishihara, K., Okada, S. 1978. Effects of stress history on cyclic behavior of sand, *Soils Found,* **18(4)**, 31–45.

Ishihara, K., Tatsuoka, F., Yasuda, S. 1975. Undrained deformation and liquefaction of sand under cyclic stresses. *Soils Found*, **15**(1), 29-44.

Knittel, L., Tafili, M., Grandas Tavera, C.E., Triantafyllidis, T. 2023. Influence of recent and long-lasting loading history on the cyclic behaviour of sand: confrontation of novel experimental results and established constitutive laws. *Sci. Rep.*, **13**(1), 4576

Liu, Z., Xue, J., Ye, J. 2021. The effects of unloading on drained cyclic behaviour of sydney sand. *Acta Geot.*, **16**(9), 2791-2804.

Suzuki, T., Toki, S. 1984. Effects of preshearing on liquefaction characteristics of saturated sand subjected to cyclic loading. *Soils Found*, **24**(2), 16-28.

Tafili, M., Knittel, L., Gauger, V. 2022. Experimentelle und numerische Untersuchungen zum Kompressionsverhalten von Sand-Schluff-Gemischen. *Geotechnik*, **45**(1), 3-15.

Wichtmann, T., Fuentes, W., Triantafyllidis, T. 2019. Inspection of three sophisticated constitutive models based on monotonic and cyclic tests on fine sand: Hypoplasticity vs. Sanisand vs. ISA. *Soil Dyn. Earth. Eng.* **124**, 172-183.

Wichtmann, T., Triantafyllidis, T. 2016. An experimental database for the development, calibration and verification of constitutive models for sand with focus to cyclic loading: part I - tests with monotonic loading and stress cycles. *Acta Geot.* **11**, 739-761.